International Journal of Mechanics and Energy (IJME)
Vol. 1, Issue 1, 2013, ISSN: 2286-5845

# Modelling and simulation study of regeneration and dehumidification stages used in solar air conditioning unit

Zied Guidara*, Wissem Zghal, Habib Ben Bacha

*Laboratory of Electro-Mechanic Systems (LASEM), National School of Engineers of Sfax (ENIS), University of Sfax (US), B.P. 1173, Road Soukra km 3.5, 3038 Sfax, TUNISIA*

Received December 3, 2012 / Accepted May 14, 2013

**Abstract:** The aim of this paper is a presentation of a new solar air conditioning unit for office spaces at Tunisia and a simulation study of the behaviour of two stages. The first one is the dehumidification stage which is mainly composed of desiccant wheel. The second one is the regeneration stage which is mainly composed of flat plate solar collector, storage tank and heat exchanger. Thus, mathematical models for each of those components are developed which are based mainly on thermal and mass balances. A finite differences method is applied to the partial differential equations. The simulation study shows that minimizing the value of the distributed hot water mass flow for the storage tank is very interesting. This can be beneficial as it reduces thermal losses and makes the heating of the inlet cold water entering the storage tank effective. In addition, increasing the value of the hot water temperature produced by flat plate solar collector is interesting because it ensures an efficient heating of the water contained in the storage tank. Finally, the studied regeneration stage can successfully ensure the regeneration of the hygroscopic wheel used in the corresponding solar air conditioning unit.

**Key words:** Air conditioning; design; desiccant wheel; flat plate solar collector; storage tank; simulation.

## 1. Introduction

In Tunisia, the sector of energy confronts many problems owed essentially to the steady increase of the rhythm of the consumption. Especially the consumption of electrical energy dedicated to the air conditioning.

Consequently the replacement of the conventional electric air conditioning by another alternative becomes a necessity. So limiting the need of the electrical energy for the air conditioning and satisfying needs in air conditioning are the main objectives to be achieved in our country. These objectives should be realized without breaking the international commitments relative to the environmental protection. Indeed, these commitments mainly intend to reduce $CO_2$ emissions, avoid the use of harmful gases to the ozone layer and to the greenhouse effect used in the conventional air conditioners.

In this context, desiccant units of air conditioning present a promising solution for air conditioning, in terms of environmental protection and energy saves. In addition, desiccant dehumidification is advantageous in handling latent heat, easy to be regenerated using low-grade energy, such as solar energy [1].

Furthermore, with conventional units of air conditioning, the dehumidification of the air is done through a cooling operation under dew point temperature [2]. Thus, the air is very cold to be pulsed in the conditioned space. This operation can be characterized as an energy consuming procedure [3] and in some cases it cannot ensure the achievement of temperature and humidity levels required by the user [4]. For temperate climates, standards configurations

*** Corresponding author:** Zied Guidara
E-mail: ziedguidara@yahoo.fr

are typically employed. However, as far as the climates in the Mediterranean countries are concerned, other configurations of desiccant processes have to be implemented [5, 6]. In fact, a block of cooling in these configurations is generally installed, before or after dehumidifying the air. The cooling, on the other hand, is obtained through the use of cooling coils that are fed by cold water which is produced by machines with sorption technique or conventional refrigerated machines.

G. Panaras et al [7] showed that the desiccant wheel is a basic element of desiccant air-conditioning systems, responsible for the dehumidification of the air. In this context, this study is done in order to verify whether the studied regeneration stage can cope successfully or not with the regeneration phenomenon of the desiccant wheel.

In this research work, a new design of a solar air conditioning unit is presented: with desiccant wheel to dehumidify the air, solar collector to produce hot water for regeneration, humidifiers for humidification and a combination of heat exchangers-humidifiers to ensure the cooling of the air without the use of machines with sorption technique or conventional refrigerated machines.

Furthermore, a modelling study which is based mainly on thermal and mass balances is developed. Thus, a simulation study of the functioning of the dehumidification stage and the regeneration stage is presented.

The remainder of this paper is organized as follows. Section 2 is dedicated to the design of the solar air conditioning unit. In section 3, the functioning of the unit is described. Section 4, presents a modelling study of the dehumidification stage and the regeneration stage. In section 5, a simulation study of the functioning of the two stages is presented. Finally, section 6 presents the main conclusion of this work.

## 2. Design of the solar air conditioning unit

The design of the solar air conditioning unit is presented in Fig. 1. Compared with standard unit, two stages responsible of the pre-cooling of the ambient air and the final cooling are added. The pre-cooling stage is mainly composed by a humidifier Hum1 and a heat exchanger Ech1. The final cooling stage is mainly composed by a humidifier Hum4 and a heat exchanger Ech4.

## 3. Description of the functioning of the unit

The principle of functioning can be described as follows:

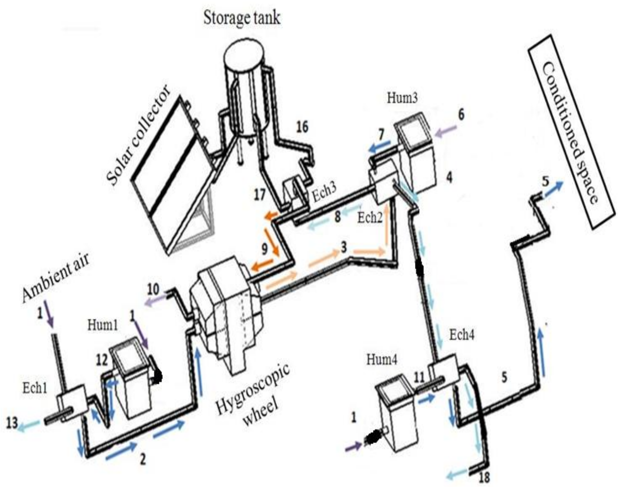


**Fig.1. Design of the solar air conditioning unit**

The ambient air is cooled close to the saturation line in a humidifier Hum1 (from 1 to12). Then, this cold air (from 12 to 13) ensures in an air/air heat exchanger Ech1 a pre-cooling of the ambient air to treat (from 1 to 2). Therefore, the first pre-cooling of the ambient air is finished. In fact, this stage is very important because it reduces the gradient of temperature which results from the dehumidification of the air which is an exothermic phenomenon. Then, the pre-cooled air is dehumidified and heated (from 2 to 3) by passing through a desiccant wheel. Later on, the dehumidified air is pre-cooled (from 3 to 4) in an air/air heat exchanger Ech2 by the air that returns from the space conditioned humidified and cooled (from 6 to 7) close to the saturation in the humidifier Hum2. Furthermore, the air is pre-cooled (from 4 to 5) by passing through an air/air heat exchanger Ech4.

Concerning the regeneration, the air that returns from the conditioned space is heated (from 8 to 9) by passing through a water/air heat exchanger Ech3 where the hot water is produced by the solar energy from a solar collector and a storage tank. Then, this hot air passes through the hygroscopic wheel to ensure its regeneration (from 9 to 10). The cycle of the conditioned air and the regenerated air is presented in Fig.2.

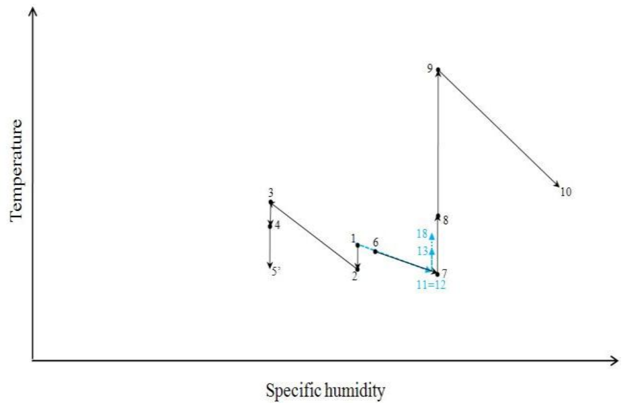


**Fig.2. Cycle of the air**

## 4. Modelling study

Four main components are studied: the flat plate solar collector, the storage tank, the heat exchanger water-air and the desiccant wheel.

### *4.1The dehumidification stage: the desiccant wheel*

The modelling of the desiccant wheel is based on mass and thermal balances for the air flow and the desiccant. The desiccant wheel is divided in two parts, the first one is for the dehumidification and the second is for the regeneration (see Fig.3). The desiccant is the silica gel.

To develop the mathematical model, these assumptions are followed:

-hysteresis in the sorption isotherm for desiccant coating is neglected and the heat of sorption (adsorption/desorption) is assumed constant,

-the canals are adiabatic, impermeable, with the same material and identical,

-the air flow is uni-directional,

-the thermodynamic properties of dry air, vapour and desiccant are uniforms and constants,

-the heat and mass coefficients between the air stream and the desiccant wall are constant along the channel.

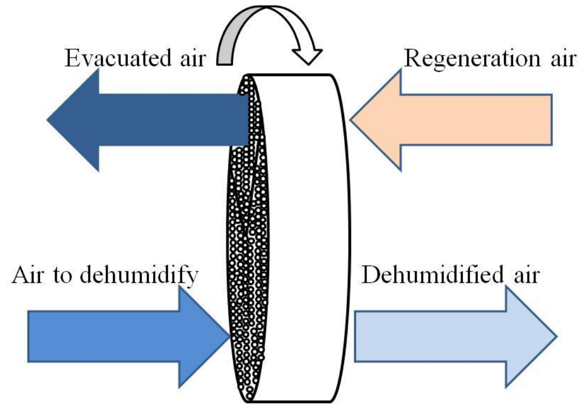


**Fig.3. The studied desiccant wheel**

Thus, the mathematical model of the desiccant wheel is written as follows:

$$A.\rho_a.C_{pa}.V.L.\frac{\partial T}{\partial x} + A.\rho_a.C_{pa}.L.\frac{\partial T}{\partial t} = h.A_{lat}.(T_p - T) \quad (1)$$

$$A.\rho_a.V.L.\frac{\partial \omega}{\partial x} + A.\rho_a.L.\frac{\partial \omega}{\partial t} = h_m.A_{lat}.(\omega_p - \omega) \quad (2)$$

$$A_d.Q_{ads}.\rho_d.L.\frac{\partial W}{\partial t} = h.A_{lat}.(T_p - T) + A_d.\rho_d.C_{pd}.L.\frac{\partial T_p}{\partial t} \quad (3)$$

$$A_d.\rho_d.L.\frac{\partial W}{\partial t} = h_m.A_{lat}.(\omega - \omega_p) \quad (4)$$

$$\omega_p = \frac{0.62188.\varphi_p}{\frac{p_{atm}}{p_{ws}} - \varphi_p} \quad (5)$$

$$p_{ws} = \exp(23.196 - \frac{3816.44}{T_p - 46.13}) \quad (6)$$

$$\varphi_p = 0.0078 - 0.05759.W + 24.16554.W^2 - 124.78.W^3 + 204.226.W^4 \quad (7)$$

*4.2 The regeneration stage*

Three main components are studied in this stage: the flat plate solar collector, the storage tank and the heat exchanger water-air.

*4.2.1Modelling of the flat plate solar collector*

The mathematical model is mainly composed by three coupled equations based on thermal balances for the glass cover, the absorber and the water (See Fig. 4).

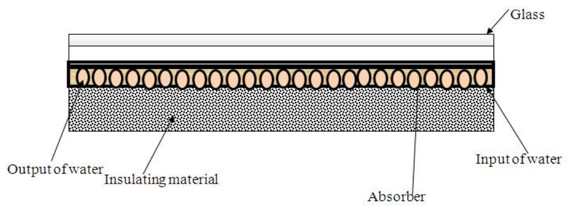


**Fig.4. Simplified figure of the studied solar collector**

To develop the mathematical model, these assumptions are followed:

-the velocity of the water is uniform,

-the water flow is uni-directional,

-the solar radiation is uniformly distributed,

-the area of the absorber, the area of the glass cover, the area of thermal exchange between the absorber and the water are equal,

-the exchanged flow by conduction between the absorber and the insulating material is neglected.

Thus, the mathematical model of the flat plate solar collector is written as follows:

$$(\alpha_v * S_v * I) + (S_a * h_{cvav} * (T_a - T_v)) + (S_a * h_{rav} * (T_a - T_v)) = m_v * C_{pv} * \frac{\partial T_v}{\partial t} + (S_v * h_{cvvam} * (T_v - T_{am})) + (S_v * h_{rvc} * (T_v - T_c)) \quad (8)$$

$$(\alpha_a * S_a * \tau_v * I) = m_a * C_{pa} * \frac{\partial T_a}{\partial t} + (S_a * h_{cvav} * (T_a - T_v)) + (S_a * h_{rav} * (T_a - T_v)) + (S_{af} * h_{cvaf} * (T_a - T_f)) \quad (9)$$

$$((m_f * C_{pf} * V_f) * \frac{\partial T_f}{\partial x}) + (m_f * C_{pf} * \frac{\partial T_f}{\partial t}) = h_{cvaf} * S_{af} * (T_a - T_f) \quad (10)$$

*4.2.2Modelling of the storage tank*

The developed mathematical model is based on thermal balances. Fig. 5 shows the studied storage tank.

To develop the mathematical model, these assumptions are followed:

-there is no exchanged flow between the storage tank and the ambient environment,

-the steady regime is established for the internal heat exchanger.

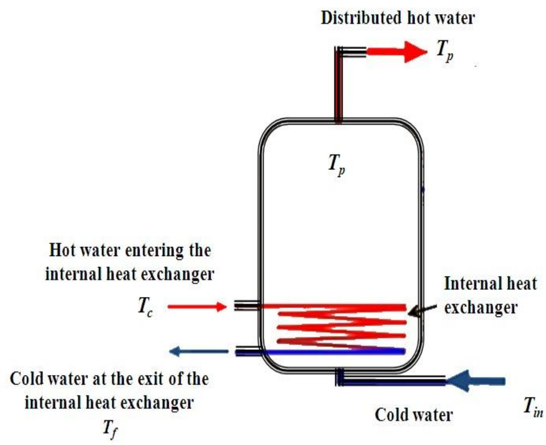


**Fig.5. Studied storage tank**

The mathematical model of the storage tank is written as follows:

$$\dot{m}_f * C_{pf} * (T_c - T_f) = \rho_f * V * C_{pf} * \frac{\partial T_p}{\partial t} + \dot{m} * C_{pf} * (T_p - T_{in}) \quad (11)$$

$$T_f = \frac{T_c - T_p}{\exp\left(\frac{h * S}{\dot{m}_f * C_{pf}}\right)} + T_p \quad (12)$$

*4.2.3Modelling of the water-air heat exchanger*

The developed mathematical model is based on the heat exchanger efficiency. Fig. 6 shows the studied heat exchanger.

To develop the mathematical model, these assumptions are followed:

-there is no exchanged flow between the heat exchanger and the ambient environment,

-the steady regime is established for the heat exchanger.

The expression of the heat exchanger efficiency is as follows [8]:

$$\eta = \frac{\dot{m}_w * C_{pw} * (T_{hw} - T_{cw})}{(\dot{m} * C_p)_{\min} * (T_{hw} - T_{ca})} = \frac{\dot{m}_a * C_{pa} * (T_{ha} - T_{ca})}{(\dot{m} * C_p)_{\min} * (T_{hw} - T_{ca})} \quad (13)$$

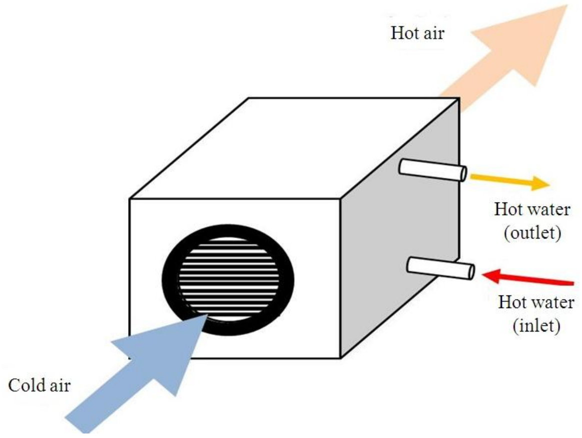


**Fig.6. Studied heat exchanger**

## 5. Simulation study

The numerical simulation is done by use of an explicit finite differential method.

*5.1 The desiccant wheel*

Numerical values used for the simulation are listed in Table 1.

**Table 1 Numerical values used for the simulation**

| Parameter | Value | Unit |
|---|---|---|
| Density of the air $\rho_a$ | 1.016 | (kg/m$^3$) |
| Specific heat of the air $C_{pa}$ | 1009 | (J/kg.K) |
| Length of one canal L | 0.2 | (m) |
| Velocity of the air V | [1.5 … 2.5] | (m/s) |
| Heat transfer coefficient h | 50 | (W/m².K) |
| Mass transfer coefficient $h_m$ | 0.04955 | (kg/m².s) |
| Adsorption heat $Q_{ads}$ | 2300.10$^3$ | (J/kg) |
| Density of the desiccant $\rho_d$ | 1129 | (kg/m$^3$) |
| Specific heat of the desiccant $C_{pd}$ | 921 | (J/kg.K) |
| Water content in the desiccant $W_{in}$ | [0.01 … 0.3] | ($kg_{H2O}/kg_{desiccant}$) |
| Space step $\Delta x$ | 0.01 | (m) |
| Time step $\Delta t$ | 0.1 | (s) |
| Silica gel wall thickness $e_p$ | 0.2.10$^{-3}$ | (m) |
| Hydraulic diameter of one canal $D$ | 2.33.10$^{-3}$ | (m) |
| Specific humidity of the air $\omega_{in}$ | [0.01 … 0.02] | ($kg_{H2O}/kg_{dry\ air}$) |
| Temperature of the air $T_{in}$ | [303 … 315] | (K) |
| Regeneration temperature $T_{reg}$ | [343 … 373] | (K) |
| Radius of the hygroscopic wheel R | 0.2 | (m) |

*5.1.1Influence of the regeneration temperature*

The influence of the regeneration temperature on the outlet temperature of the dehumidified air is presented in Fig. 7.

The results show that the higher the regeneration temperature is, the higher is the temperature gradient between the air to dehumidify and the dehumidified air. But for the four regeneration temperatures 70 °C, 80 °C, 90 °C and 100 °C used in the studied cases, the difference between the gradients of temperature does not exceed 2°C.

The influence of the regeneration temperature on the outlet specific humidity of the dehumidified air is presented in Fig. 8.

The results show that the higher the regeneration temperature is, the higher is the specific humidity gradient between the air to dehumidify and the dehumidified air.

But for the four regeneration temperatures 70 °C, 80 °C, 90 °C and 100 °C used in the studied cases, the difference between the gradients of specific humidity does not exceed 0.0005 $kg_{H2O}/kg_{dry\ air}$. This can be beneficial as it allows the use of a regeneration temperature which is relatively low 70 °C.

Thus, minimizing the value of the regeneration temperature is interesting because it can facilitate the cooling of dehumidified air in solar air conditioning unit and simplify the design of the regeneration stage.

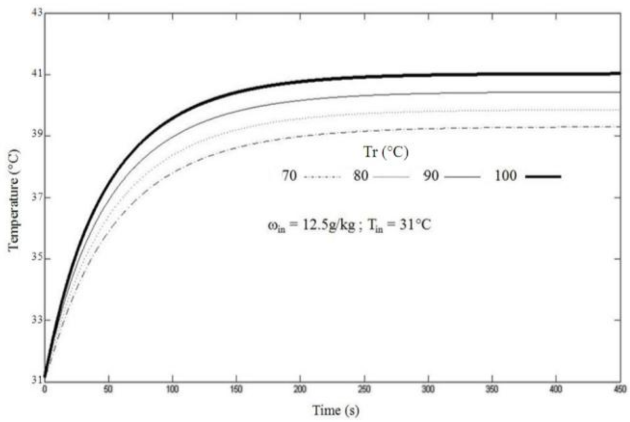


**Fig. 7. Influence of regeneration temperature on dehumidified air temperature**

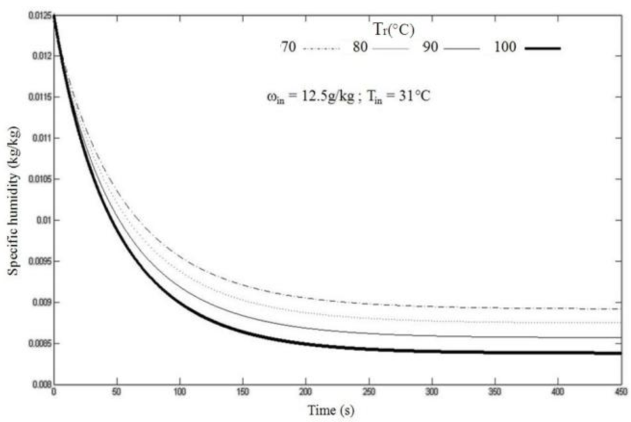


**Fig. 8. Influence of regeneration temperature on dehumidified air humidity**

*5.1.2Influence of the specific humidity of the air to dehumidify*

The influence of the specific humidity on the outlet temperature of the dehumidified air is presented in Fig. 9.

The results corresponding to the five values of specific humidity of the air to be dehumidified 10 g/kg, 12.5 g/kg, 15 g/kg, 17.5 g/kg and 20 g/kg, show that the higher the specific humidity of the air to dehumidify is, the higher is the temperature gradient between the air to dehumidify and the dehumidified air.

So, minimizing the value of the specific humidity of the air to dehumidify is very interesting. This can be beneficial as it facilitates the cooling of dehumidified air in desiccant solar air conditioning unit.

The influence of the specific humidity on the outlet specific humidity of the dehumidified air is presented in Fig. 10.

The results corresponding to the five values of the specific humidity of the air to dehumidify 10 g/kg, 12.5 g/kg, 15 g/kg, 17.5 g/kg and 20 g/kg, show that the higher the specific humidity of the air to dehumidify is, the higher is the specific humidity of the dehumidified air.

So, minimizing the value of the specific humidity of the air to dehumidify is very interesting. This can be beneficial as it facilitates the cooling of dehumidified air in desiccant solar air conditioning unit.

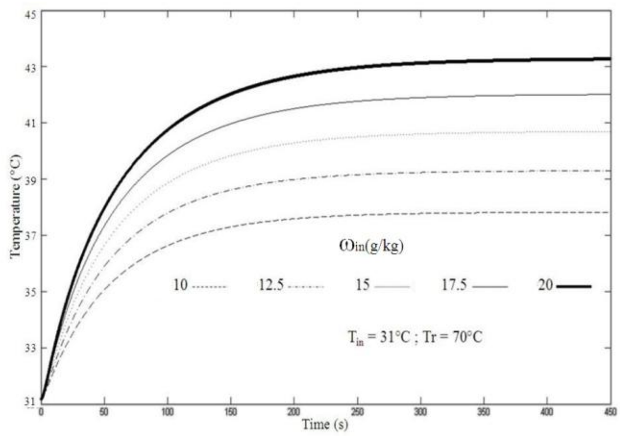


**Fig. 9. Influence of specific humidity of the air to treat on dehumidified air temperature**

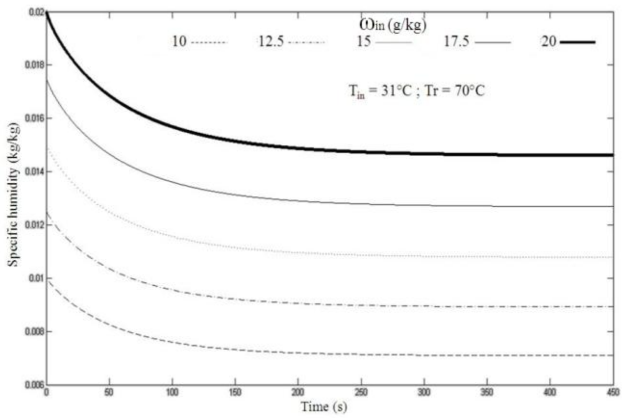


**Fig. 10. Influence of specific humidity of the air to treat on dehumidified air humidity**

*5.1.3Influence of the temperature of the air to dehumidify*

The influence of the temperature of the air to dehumidify on the outlet temperature of the dehumidified air is presented in Fig. 11.

The results corresponding to the four values of the temperature of the air to dehumidify between 30 °C et 42 °C show that the higher the temperature of the air to dehumidify is, the higher is the temperature of the dehumidified air.

Therefore, minimizing the value of the temperature of the air to dehumidify is very interesting. This can be beneficial as it facilitates the cooling of dehumidified air in desiccant solar air conditioning unit.

The influence of the temperature of the air to dehumidify on the outlet specific humidity of the dehumidified air is presented in Fig. 12.

The results show that the lower the temperature of the air to dehumidify is, the higher is the specific humidity gradient between the air to dehumidify and the dehumidified air.

Therefore, minimizing the value of the temperature of the air to dehumidify is very interesting. This can be beneficial as it facilitates the cooling of dehumidified air in desiccant solar air conditioning unit.

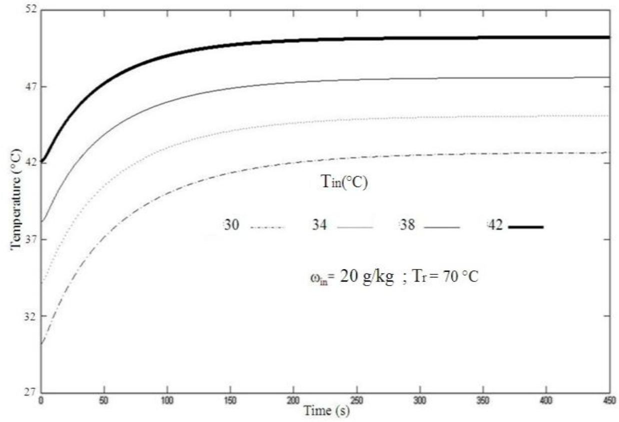


**Fig. 11. Influence of temperature of the air to treat on dehumidified air temperature**

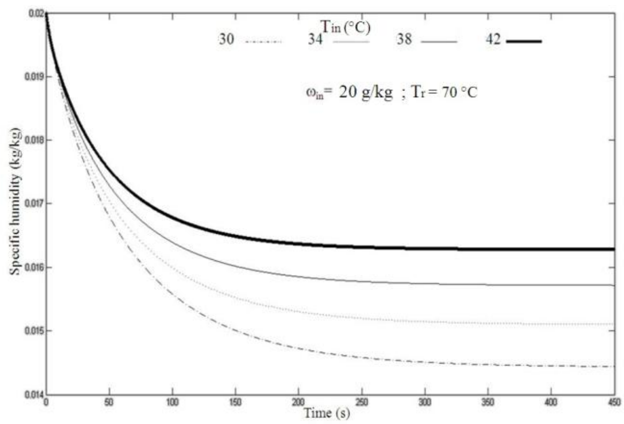


**Fig. 12. Influence of temperature of the air to treat on dehumidified air humidity**

*5.2 The flat plate solar collector*

Numerical values used for the simulation are listed in Table 2.

**Table 2 Numerical values used for the simulation of the flat plate solar collector**

| Parameter | Value | Unit |
|---|---|---|
| Space step $\Delta x$ | 0.1 | (m) |
| Time step $\Delta t$ | 0.1 | (s) |
| Velocity of water flow $V_f$ | [0.25 , 2] | (m/s) |
| Solar radiation $I$ | [500 , 870] | (W/m²) |
| Transmission coefficient of the glass cover $\tau_v$ | 0.8 | |
| Absorption coefficient of the | 0.9 | |

| | | |
|---|---|---|
| absorber $\alpha_a$ | | |
| Wind velocity $V_v$ | [3 , 6] | (m/s) |
| Internal diameter interne of one canal $d_i$ | $1.10^{-2}$ | (m) |
| Angle of inclination of the flat plate solar collector $\Phi$ | $\pi/4$ | (rad) |
| Width of the absorber $l$ | 1 | (m) |
| Length of the solar collector $L$ | 2 | (m) |

*5.2.1Influence of solar radiation*

Fig. 13 presents the influence of solar radiation on the temperature of hot water at the exit of solar collector. The results show that the higher the value of solar radiation is, the higher the temperature of the hot water at the exit of the flat plate solar collector is.

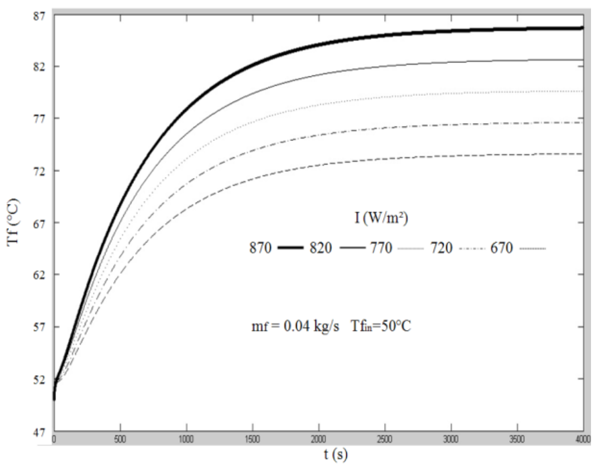


**Fig. 13. Influence of solar radiation**

*5.2.2Influence of initial temperature of water*

Fig. 14 shows the profile of the temperature of hot water at the exit of solar collector for five values of initial temperatures of water entering the solar collector. The results show that the smaller the value of initial temperature of water entering the solar collector is, the higher the difference between the initial temperature and the final temperature of hot water is.

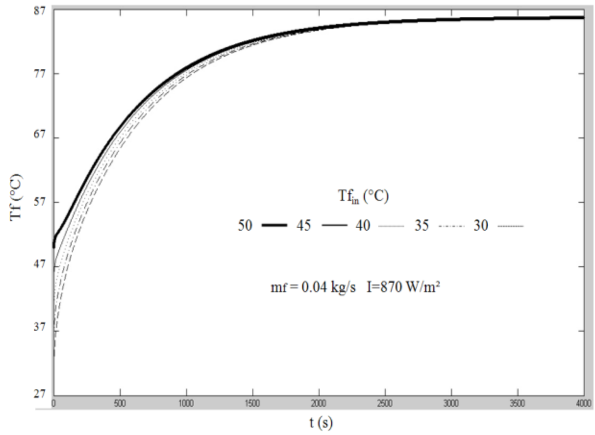


**Fig. 14. Influence of initial temperature of water**

*5.3 The storage tank*

Numerical values used for the simulation are listed in Table 3.

**Table 3 Numerical values used for the simulation of the storage tank**

| Parameter | Value | Unit |
|---|---|---|
| Density of water $\rho_f$ | 1000 | (kg/m$^3$) |
| Time step $\Delta t$ | [0.2 , 1] | (s) |
| Water specific heat $C_{pf}$ | 4182 | (J/kg.K) |
| Volume of the storage tank $V$ | 1 | m$^3$ |
| Mass flow of the water entering the internal heat exchanger $m_f$ | 0.04 | kg/s |
| Mass flow of the Distributed hot water $\dot{m}$ | [0.01, 0.03] | kg/s |
| Temperature of hot water entering the internal heat exchanger $T_c$ | [335, 355] | K |
| Temperature of cold water entering the storage tank $T_{in}$ | [303, 323] | K |

*5.3.1Profile temperature of distributed hot water*

Fig. 15 shows the influence of inlet cold water temperature on distributed hot water temperature. The results show that the higher the value of inlet cold water temperature is, the higher the value of distributed hot water temperature is.

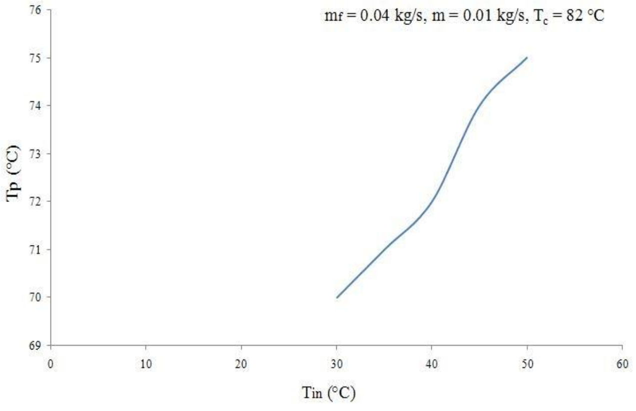


**Fig. 15. Profile temperature of distributed hot water**

*5.3.2. Influence of distributed hot water mass flow*

Fig. 16 shows the influence of distributed hot water mass flow on the difference between distributed hot water temperature and inlet cold water temperature. The results show that the higher the value of distributed hot water mass flow is, the smaller the value of the difference between distributed hot water temperature and inlet cold water temperature is. So, minimizing the value of distributed hot water mass flow is interesting. This can be beneficial as it facilitates the heating of the inlet cold water and makes the heating effective.

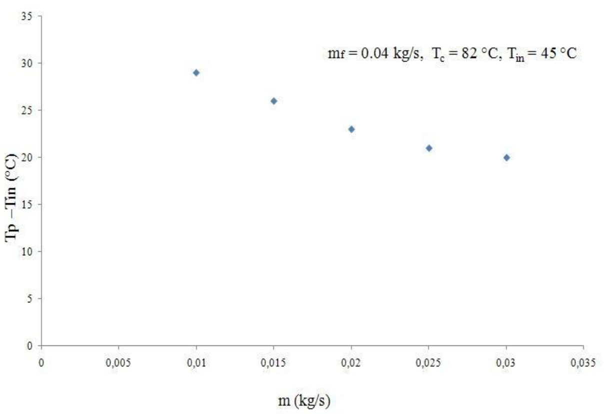


**Fig. 16. Influence of distributed hot water mass flow**

*5.4 The regeneration stage*

Fig. 17 presents the studied regeneration stage composed by the flat plate solar collector, the storage tank and the heat exchanger water-air Ech3.

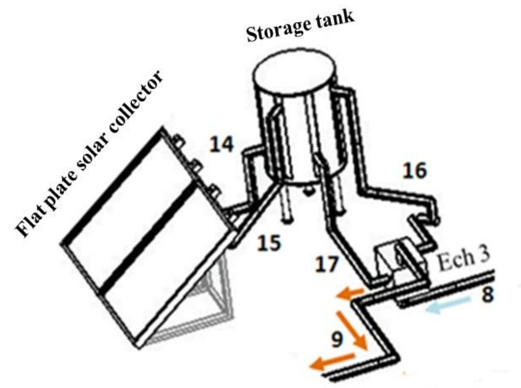


**Fig.17. Regeneration stage**

Inlet/outlet points of the regeneration stage are listed in Table 4.

**Table 4 Inlet/outlet points of the regeneration stage**

| Component of the regeneration stage | Inlet | Outlet |
|---|---|---|
| Flat plate solar collector | Point 14 | Point 15 |
| Storage tank | Point 17 | Point 16 |
| | Point 15 | Point 14 |
| Heat exchanger Ech3 | Point 16 | Point 17 |
| | Point 8 | Point 9 |

Note that points 14, 15, 16 and 17 are crossing points of water flow, while points 8 and 9 are crossing points of air flow.

Numerical values used for the simulation of the regeneration stage are listed in Table 5.

**Table 5 Numerical values used for the simulation of the regeneration stage**

| Parameter | Value | Unit |
|---|---|---|
| Temperature of the air to heat T8 | 30 | °C |
| Solar radiation I | 870 | W/m² |
| Density of the air $\rho_a$ | 1,016 | kg/m$^3$ |
| Volume flow of the air $D_a$ | 150 | m$^3$/h |
| Ambient temperature $T_{amb}$ | 37 | °C |
| Mass flow of the air to heat $m_8$ | 0.0423 | kg/s |
| Mass flow of the heated air $m_9$ | 0.0423 | kg/s |

| | | |
|---|---|---|
| Mass flow of the water entering the flat plate solar collector $m_{14}$ | 0.04 | kg/s |
| Mass flow of the hot water produced by the flat plate solar collector $m_{15}$ | 0.04 | kg/s |
| Mass flow of the hot water entering the heat exchanger Ech 3 $m_{16}$ | 0.019 | kg/s |
| Mass flow of the hot water at the exit of the heat exchanger Ech 3 $m_{17}$ | 0.019 | kg/s |

Table 6 represents numerical values obtained through the simulation of the functioning of the regeneration stage for points 9, 14, 15, 16 and 17.

Thus, based on the previously studied case, the regeneration stage can produce hot air with a temperature $T_9$ equal to 67 °C. This value seems to be enough to ensure the regeneration of the hygroscopic wheel used in the corresponding solar air conditioning unit.

**Table 6 Numerical values obtained through the simulation of the functioning of the regeneration stage**

| Parameter | Value | Unit |
|---|---|---|
| Temperature of the heated air $T_9$ | 67 | °C |
| Temperature of the water entering the flat plate solar collector $T_{14}$ | 72 | °C |
| Temperature of the hot water produced by the flat plate solar collector $T_{15}$ | 85 | °C |
| Temperature of the hot water entering the heat exchanger Ech 3 $T_{16}$ | 70 | °C |
| Temperature of the hot water at the exit of the heat exchanger Ech 3 $T_{17}$ | 50 | °C |

## 6. Conclusion

A design of a solar air conditioning unit is developed where the cooling operation is ensured mainly by the use of a humidifier and a heat exchanger. Furthermore a modelling study is detailed for the regeneration and the dehumidification stage.

As seen through the simulation study, minimizing the value of the distributed hot water mass flow for the storage tank is very interesting. This can be beneficial as it reduces thermal losses and makes the heating of the inlet cold water entering the storage tank effective.

In addition, increasing the value of the hot water temperature produced by flat plate solar collector is interesting because it ensures an efficient heating of the water contained in the storage tank.

Furthermore, increasing the value of the initial temperature of water entering the flat plate solar collector is interesting because it ensures an efficient solar heating.

Finally, the studied regeneration stage can successfully ensure the regeneration of the hygroscopic wheel used in the corresponding solar air conditioning unit.

## References

[1] Y. J. Dai, R. Z. Wang, H. F. Zhang, J. D. Yu, Use of liquid desiccant cooling to improve the performance of vapour compression air conditioning, Appl Therm Eng, 21 (2001) 1185–1202.

[2] P.L. Dhar, S.K. Singh, Studies on solid desiccant based hybrid air-conditioning systems, Appl Therm Eng, 21 (2001) 119-134.

[3] Seiichi Yamaguchi, Jongsoo Jeong, Kiyoshi Saito, Hikoo Miyauchi, Masatoshi Harada, Hybrid liquid desiccant air-conditioning system: Experiments and simulations, Appl Therm Eng, 31 (2011) pp. 3741-3747.

[4] Sand JR, Fischer JC, Active desiccant integration with packaged rooftop HVAC equipment, Appl Therm Eng, 25 (2005) 3138-3148.

[5] Hans-Marting Henning, Solar assisted air conditioning of buildings – an overview, Appl Therm Eng, 27(2007) 1734–1749.

[6] Chaouki Ali; Habib Ben Bacha; Mounir Baccar; Aref Y. Maalej, Dynamic modelling and simulation of a new air conditioning prototype by solar energy, Renewable Energy, 32 (2007) 200-215.

[7] G. Panaras, E. Mathioulakis, V. Belessiotis, Solid desiccant air conditioning systems -Design parameters, Energy, 36 (2011) 2399-2406.

[8] Allan D. Kraus, Heat Exchangers, Heat Transfer Handbook, Chapter 11, (2003).